

Influence of vertical load on the lateral response of piles in sand

S. Karthigeyan^a, V.V.G.S.T. Ramakrishna^a, K. Rajagopal^{b,*}

^a Central Building Research Institute, Roorkee 247 667, India

^b Department of Civil Engineering, Geotechnical Engineering Division, Indian Institute of Technology Madras, Chennai 600 036, India

Received 26 April 2005; received in revised form 28 October 2005; accepted 16 December 2005

Available online 2 May 2006

Abstract

Pile foundations are often subjected to both vertical and lateral loads. The current design practices assume that the effect of these two loads is independent of each other and hence the pile design is carried out separately for vertical and lateral loads. The conventional methods for analysis of piles based on sub-grade reaction methods also do not account for the interaction between the vertical and lateral loads. The influence of vertical loads on the lateral response of piles installed in sandy soils is brought out in this paper through 3-dimensional finite element analyses. In the numerical model, the pile was treated as a linear elastic material and the soil was idealized using the Drucker–Prager constitutive model with a non-associated flow rule. The results from the analysis of single piles under pure lateral loads and combined vertical and lateral loads are presented in this paper. The influence of related parameters, viz. sequence of load application, shear strength (angle of internal friction and dilation angle) of soil, pile head fixity and pile slenderness (L/B) ratio have also been studied in the paper.

© 2006 Elsevier Ltd. All rights reserved.

Keywords: Pile; Lateral deflection; 3-dimensional finite element analysis; Constitutive model; Sand

1. Introduction

Pile foundations are extensively used to support various structures built on loose/soft soils, where shallow foundations would undergo excessive settlements or have low bearing capacity. These piles are not only used to support vertical loads, but also lateral loads and combination of vertical and lateral loads. According to current day practice, piles are independently analyzed first for the vertical load to determine their bearing capacity and settlement and for the lateral load to determine the flexural behaviour. This approach is valid only for small lateral loads, however, in case of coastal/offshore applications, the lateral loads are significantly high of the order of 10–20% of the vertical loads and in such cases, studying the interaction effects due to combined vertical and lateral loads is essential, which calls for a systematic analysis.

Several investigators have attempted to study the behaviour of piles and pile groups under pure lateral loads [12,16,17]. Besides, with the advent of latest generation computers, it is now possible to investigate the effects due to non-linearity and elasto-plasticity of soil medium, asymmetric loading on piles etc. using 3-dimensional finite element analysis [4,8,11,14,20–23]. However, there is hardly any concerted effort to study the influence of vertical load on the lateral response of piles and the literature on combination of vertical and lateral loads is scanty. The limited information on this aspect based on the analytical investigations [6,7,18] reveals that for a given lateral load, the presence of vertical load increases the lateral deflection. However, laboratory [1,9] and field investigations [2,10,13,19,24] suggest a decrease in lateral deflection under the presence of vertical loads. Anagnostopoulos and Georgiadis [1] have reported that the modified status of soil stresses and local plastic volume changes in the soil continuum under combined vertical and lateral loads cannot be accounted for in general by the conventional subgrade reaction and elastic half space methods of analysis.

* Corresponding author. Tel.: +91 44 2257 9298; fax: +91 44 2257 8281.
E-mail address: gopalkr@iitm.ac.in (K. Rajagopal).

Therefore, they suggest using a nonlinear 3-dimensional finite element technique for analyzing this problem. Trochanis et al. [20] attempted to study the behaviour of a pile under combined vertical and lateral loads based on 3-dimensional nonlinear finite element method. The emphasis was mainly focused on the influence of lateral load on the axial response of a pile rather than the influence of vertical load on the lateral response of piles. However, since piles are not often structurally designed to resist lateral loads, the lateral response of piles is more critical and interesting for design engineers. In view of the above stated issues, the present paper focuses on the influence of vertical load on the lateral response of piles. The details of the numerical model, the parameters studied and the verification of the developed model against some field cases are discussed.

2. Numerical model

The 3-dimensional finite element program GEOFEM3D developed by the authors has been used to analyze the pile–soil interaction problem. The program is supported by a pre-processor to develop 3-dimensional meshes consisting of 8-node or 20-node brick elements, 8 or 16-node zero thickness type interface elements as well as a post-processing programme that is capable of plotting the original mesh, deformed mesh, displacement vectors, extracting nodal displacements and element stresses along a line/selected plane etc.

2.1. Validation of the numerical model employed in the program

The validity of the numerical model employed in the program was verified by back predicting the pile load test data from two different published cases, one with respect to a short rigid pile and another for a long flexible pile. The details of these two cases are presented in the following sub-sections.

2.1.1. Case study – I [10]

The length and diameter of the concrete test pile considered by Karasev et al. [10] were 3 m and 600 mm, respectively. The pile was installed in a soil strata consisting of very stiff sandy loam in the top 6 m and underlain by a sandy clay of lower stiffness of more than 7 m thickness. The shear strength parameters of the topsoil layer were reported as $c = 18$ kPa and $\phi = 18^\circ$ and that of the bottom layer as $c = 24$ kPa and $\phi = 14^\circ$. The Young's modulus and the Poisson's ratio of the top soil were taken as 25,000 kPa and 0.35, respectively based on empirical correlations [3]. The soil in the bottom layer was assumed to have Young's modulus of 20,000 kPa and Poisson's ratio of 0.40. The dilation angle of the soil in both layers was assumed to be 0° . The field tests were conducted by first loading the pile in the vertical direction and then the horizontal loads were applied while the vertical load was kept

constant. The same sequence of load application was followed in the current finite element analysis. The behaviour of the soil was modelled using the Drucker–Prager constitutive model. This model has been preferred over other models in view of its adaptability to define the failure criterion with the use of simple physical properties like ' c ' and ' ϕ '. The pile and the soil were modelled using 20 node brick elements. Using symmetry, only half of the pile was considered in the analysis. The comparison between the finite element predicted and the reported data is shown in Fig. 1. The finite element analysis diverged at a load increment of 110 kN which can be considered as numerical collapse load. The numerical analysis was stopped at this stage. The difference in the deformations is because the soil stiffness properties were derived approximately through empirical correlations based on the soil description. Nevertheless the comparison can be considered as good for all practical design purposes.

2.1.2. Case study – II [5]

Comodromos [5] has reported the response of a 52 m long, 1 m diameter bored pile under lateral loads installed at a bridge site in Greece. The subsoil at the site consists of a thick upper soft silty clay layer with thin layers of loose sand extending to a depth of 36 m. Below this, a medium stiff clay layer of 12 m thickness existed which is followed by a very dense sandy gravel layer up to the bottom of the borehole. The behaviour of the test pile is analysed by finite element analysis using the program GEOFEM3D. The mesh consisted of 20-node isoparametric continuum brick elements and 16-node zero-thickness joint elements to model the interfaces between the pile and soil. The properties of various soil layers and the finite element mesh are similar to those reported by Comodromos [5]. The behaviour of soil layers was modelled using the Drucker–Prager constitutive model. Using symmetry, only half of the pile

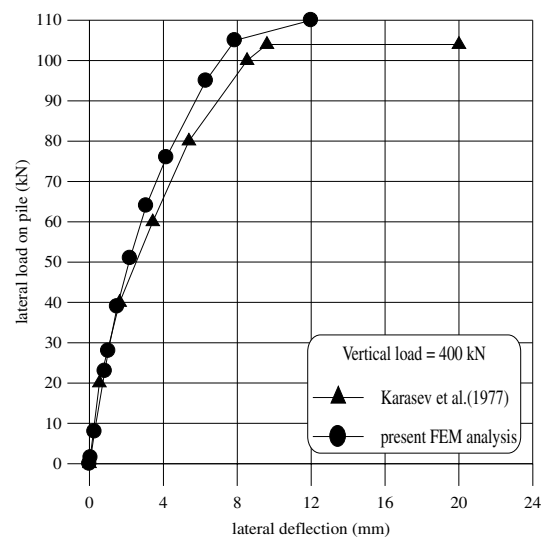


Fig. 1. Comparison of finite element results with field test data of Karasev et al. [10].

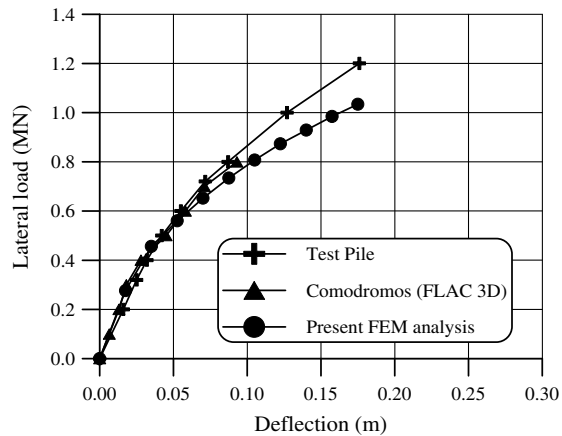


Fig. 2. Comparison of finite element results with field and numerical data of Comodromos [5].

was considered in the analysis. The same sequence of load application used in the field test was followed in the current finite element analysis. The comparison between the finite element predictions and the reported data is shown in Fig. 2. Up to a lateral displacement equal to about 7% of the pile diameter, the difference between the measured and predicted pile loads is less than 10%. At a larger displacement equal to 17.5% of the pile diameter, the difference between the two increases to approximately 13%. This percentage error is acceptable in view of the many uncertainties in the soil properties assumed in the analysis. It may be noted that the numerical solution reported by Comodromos [5] was stopped at a displacement of about 0.09B, while the present numerical analyses was continued to almost 17% of the pile width.

Thus, it can be noted that the proposed numerical scheme is reasonably accurate for pile–soil interaction problems over a wide range of deflections for both short and long piles.

3. Parametric studies

The finite element program was used to perform a series of analyses on piles subjected to both vertical and lateral loads in loose and dense sands. The analyses were performed to study the influence of vertical loads on the lateral response of piles. The details of the finite element model and the results are discussed in the following sections.

3.1. Mesh details

Fig. 3 shows the schematic 3-d finite element mesh discretization of the pile–soil continuum. Based on symmetry, only half of the pile section in the direction of the lateral load is analysed (in Fig. 3, lateral load is applied along X-axis). The pile and soil continuum are discretized by using 20-node isoparametric brick elements and the interface between the pile and soil has been modelled using 16-node joint elements of zero thickness to represent possi-

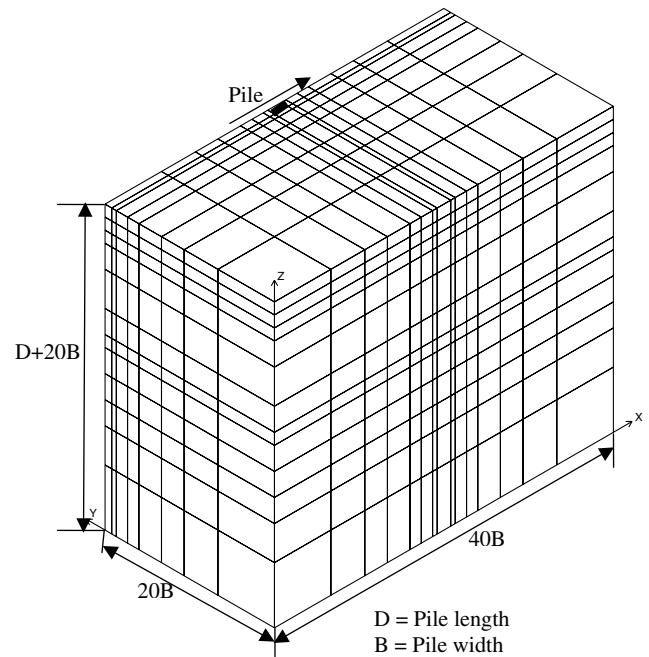


Fig. 3. Typical mesh for three-dimensional finite element analyses.

ble slip and separation between the pile and the soil. Yang and Jeremic [23] reported that 20-node brick elements exhibit high accuracy, even for high aspect ratios and can accurately model the flexural behaviour of piles. Hong et al. [8] reported that due care has to be taken while developing finite element meshes in order to obtain the best numerical results. Analyses were performed with several trial meshes with increasing refinement until the displacements did not change with more refinement. The aspect ratios of elements used in the mesh ranged from 0.5 near the pile head to about 5 near the boundaries of the finite element mesh. The mesh dimensions are shown in Fig. 3. All the nodes on the lateral boundaries are restrained from moving in the normal direction to the respective surfaces representing rigid, smooth lateral boundaries. The nodes at the bottom surface are restrained in all the three directions representing rough, rigid bottom surface. Typically, the finite element meshes consisted of approximately 7100 nodes, 1200 20-node brick elements and 40 16-node interface elements.

3.2. Pile–soil details

The pile was treated as a linear elastic material and the behaviour of soil has been idealized using the Drucker–Prager perfectly plastic constitutive model with a non-associated flow rule. The yield surface for this model has the form $F = \alpha J_1 + \sqrt{J_{2d}} - k$, in which J_1 is the first invariant of the stress tensor, J_{2d} is the second invariant of the deviatoric stress tensor and α , k are the material constants expressed in terms of the well-known soil shear strength parameters ‘ c ’ and ‘ ϕ ’ by matching the circle with the outer corners of Mohr–Coulomb yield surface. This model might

over predict the friction angle for an extension stress path, however the influence is limited only to the zone behind the pile near the interface, as reported by other investigators [23].

During plastic flow, the constitutive matrix was first formed based on the current tangent modulus and the Poisson's ratio for elastic state. Then a correction was applied to obtain the elastic–plastic constitutive matrix. The stresses are corrected back to the yield surface along the flow direction (normal to the potential surface defined by the dilation angle ψ) as described by Nayak and Zienkiewicz [15].

3.3. Analysis scheme

The finite element analyses have been performed in two stages. In the first stage, the in situ stresses were initialized in the soil by performing a dummy analysis using a modified Poisson's ratio expressed in terms of the at-rest earth pressure coefficient K_0 as $K_0/1 + K_0$. The value of K_0 itself was obtained as $K_0 = 1 - \sin \phi$. At the end of this stage, all deformations and strains are set to zero to define the datum level for further analysis. During this stage of analysis, both the pile and the soil elements were assigned the same material properties (Young's modulus, Poisson's ratio and unit weight) so as not to generate any extraneous shear stresses.

During the second stage of analysis, the actual properties of the soil and pile elements were assigned to them. The set of pile–soil properties considered are shown in Table 1. The soil properties for loose and dense states were arrived at using correlations between SPT N -values and Young's modulus for soil, Bowles [3]. The interfaces were assumed to have zero cohesive strength and the friction angle was assumed to be 2/3 of the friction angle of the surrounding soil. Initially, the interface elements were assumed to have very high normal and shear stiffness values of 10^6 kN/m²/m. After the shear failure, the shear stiffness was set to a small value of 0.1% of the initial stiffness. When the interface is in tension, the normal stiffness was reduced to 0.1% of the initial value to allow for separation between the soil and pile.

In the second stage of analysis, the external loads were applied in small increments in several load steps. Within each load step, several iterations were performed to satisfy the equilibrium equations. The iterations were continued at

each load step until the norms of the out-of-balance force and incremental displacements were less than 0.5% or until 50 iterations are completed. The analyses were performed using a partial Newton–Raphson scheme by updating the stiffness matrix at the first iteration of each load step.

4. Results and discussion

A series of three-dimensional finite element analyses have been carried out to study the behaviour of piles under pure lateral loads and the influence of vertical load on the lateral response of piles. Several factors were considered in this parametric study namely, (i) the method of loading (ii) the soil parameters (iii) the pile head fixity and (iv) the pile slenderness ratio (L/B). The results obtained from this investigation with reference to various parameters are presented as follows.

4.1. Influence of method of loading

In the present analysis, the vertical load on the pile was applied in two different ways, (i) simultaneously with the lateral load and (ii) prior to the lateral load. In the first case, both vertical load and lateral displacements at the pile head were applied simultaneously in small increments in each load step. This case is referred to in this paper as Simultaneously Applied Vertical and Lateral loads (SAVL) case. In the second case, vertical loads were applied first and then in the second stage, equal lateral displacement increments were applied on the nodes corresponding to the pile head while the vertical loads were kept constant. The reaction forces developed at the nodes were used to calculate the lateral forces corresponding to the applied lateral displacements. The analysis in the lateral direction was performed using displacement control (rather than load control) so as to know the loads developed at various lateral displacement levels as a percentage of pile size. The second case is referred to in the paper as Vertical load Prior to Lateral load (VPL) case.

The ultimate vertical load (V_{ult}) capacity of a single pile was evaluated a priori by separate numerical analyses. Then the response of piles under combined loading was analyzed separately with the vertical load equal to zero (pure lateral load case), $0.2V_{ult}$, $0.4V_{ult}$, $0.6V_{ult}$ and $0.8V_{ult}$.

Figs. 4 and 5 show the lateral load vs. deflection relationship of a pile in loose sand ($\phi = 30^\circ$) corresponding

Table 1
Properties of pile and soil

Pile details	Soil details	
	Loose sand	Dense sand
Size: 1200 × 1200 mm square	Friction angle (ϕ) = 30°	$\phi = 36^\circ$
Length: 10 m	Dilation angle (ψ) = 0–10°	$\psi = 0–12^\circ$
Type of pile: concrete	Unit weight (γ) = 18 kN/m ³	$\gamma = 20$ kN/m ³
Grade of concrete: M25	Young's modulus (E_s) = 20 MPa	$E_s = 50$ MPa
Young's modulus E_p : 25,000 MPa	Poisson's ratio (μ_s) = 0.30	$\mu_s = 0.30$
Poisson's ratio μ_p : 0.15	Earth pressure (K_0) = 0.5	$K_0 = 0.42$

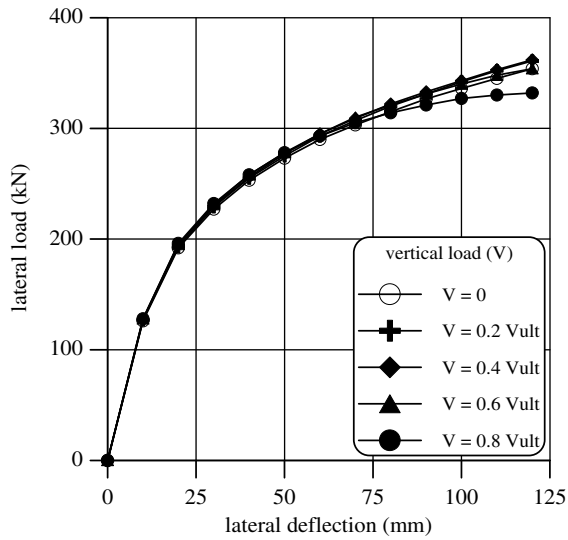


Fig. 4. Lateral load–deflection behaviour of a pile in loose sand for the SAVL case.

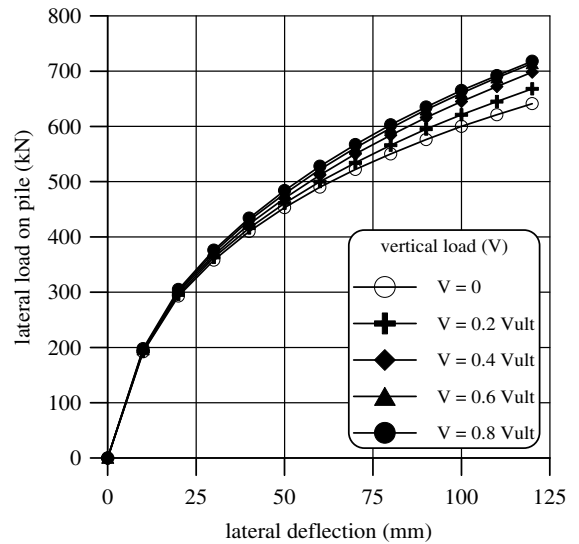


Fig. 6. Lateral load–deflection behaviour of a pile in dense sand for the SAVL case.

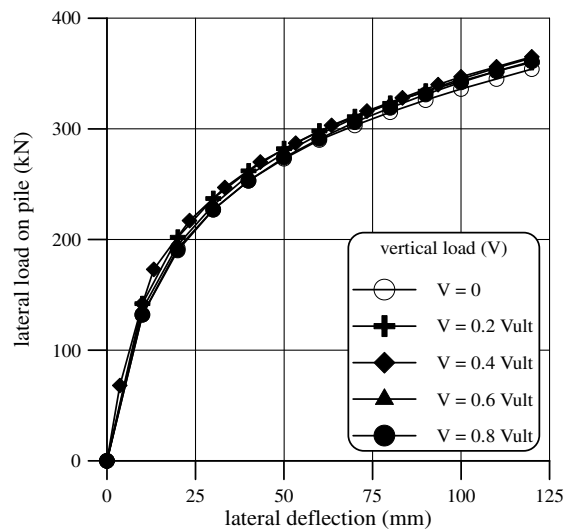


Fig. 5. Lateral load–deflection behaviour of a pile in loose sand for the VPL case.

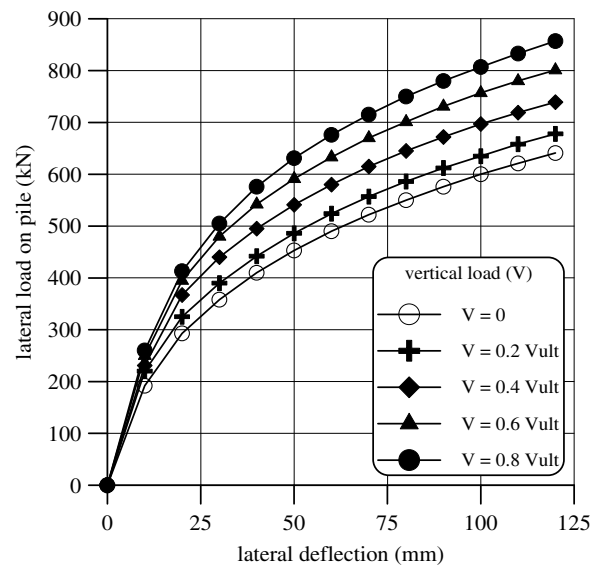


Fig. 7. Lateral load–deflection behaviour of a pile in dense sand for the VPL case.

to the SAVL and VPL cases, respectively. It is seen from these figures that the vertical load has only a marginal influence on the lateral response of piles in the case of loose sands for both the SAVL and VPL cases. The response of piles in dense sands ($\phi = 36^\circ$) for both the SAVL and VPL cases is shown in Figs. 6 and 7. The influence of vertical load on the lateral response of a pile is more significant in the VPL case than in the SAVL case for dense sand.

5. Influence of soil parameters

A quantity termed as the Percentage Improvement in lateral Capacity (PIC) has been defined to measure the influence of vertical loads on the lateral response of piles in loose and dense sands.

$$PIC = \frac{LCWV - LCNV}{LCNV} \times 100;$$

where ‘LCWV’ is the Lateral load Capacity With Vertical load and ‘LCNV’ is the Lateral load Capacity under pure lateral load (without vertical load). The PIC values from different analyses have been summarized in Tables 2 and 3.

It could be observed from Table 2 for the SAVL case that, in the case of loose sands, the PIC values increase with the vertical load up to 2.5% at lateral deflections equal to 0.05B (i.e., 60 mm). There is even a decrease in lateral capacities for vertical loads beyond 0.6 V_{ult} at lateral deflections equal to 0.1B (i.e., 120 mm). However, on the other hand, there is a considerable increase in lateral capacities in the case of dense sands as illustrated in Tables 2 and 3. It is clear

Table 2
Percentage Improvement in the lateral Capacity (PIC) with respect to different vertical load levels in the SAVL case

Vertical load in terms of V_{ult}	Lateral load at deflection of 0.05B		PIC at deflection of 0.05B		Lateral load at deflection of 0.1B		PIC at deflection of 0.1B	
	Loose	Dense	Loose	Dense	Loose	Dense	Loose	Dense
0	273	453	–	–	354	641	–	–
0.2	275	461	+0.7	+1.7	361	668	+1.9	+4.2
0.4	277	470	+1.4	+3.7	363	698	+2.5	+8.9
0.6	280	478	+2.5	+5.5	354	714	0.0	+11.4
0.8	278	484	+1.8	+6.8	330	718	–6.8	+12.0

Table 3
Percentage Improvement in the lateral Capacity (PIC) with respect to different vertical load levels in the VPL case

Vertical load in terms of V_{ult}	Lateral load at deflection of 0.05B		PIC at deflection of 0.05B		Lateral load at deflection of 0.1B		PIC at deflection of 0.1B	
	Loose	Dense	Loose	Dense	Loose	Dense	Loose	Dense
0	317	453	–	–	398	641	–	–
0.2	326	486	+2.8	+7.3	410	678	+3.0	+5.8
0.4	334	547	+5.3	+20.7	420	740	+5.5	+15.4
0.6	346	591	+9.1	+30.4	434	801	+9.0	+24.9
0.8	362	631	+14.2	+39.3	453	857	+13.8	+33.7

that in the case of dense sands, there is increase in the PIC value of 1.7–6.8% corresponding to deflections of 0.05B and a significant increase of the order of 12% at higher deflections of 0.1B under the presence of vertical loads.

Similarly from Table 3 for the VPL case, it can be noted that, in the case of loose sands, there is an increase in PIC with increasing vertical loads of 2.8–14.2% at both the deflection levels considered, whereas in the case of dense sands, the increase in PIC value is much higher and lies in the range of 5.8–39.3%. From the above tables and discussion, it is clear that the lateral capacities of piles in sands improve in general under the presence of vertical loads. This could be attributed to the following: (i) under the influence of vertical loads, higher vertical soil stresses

develop in the soil along the pile surface leading to higher lateral stresses in the soil, (ii) higher lateral stresses in turn mobilize larger friction forces along the length of the pile.

This is further illustrated through lateral soil stresses developed in front of the pile at different vertical load levels for a lateral deflection equal to 0.1B, as shown in Figs. 8a and 8b for loose and dense sands under VPL case, respectively. It is clear that the lateral soil stresses are not much affected by vertical loads in the case of loose sand as shown in Fig. 8a. On the other hand, the lateral stresses for dense sands increase because of the presence of vertical load as illustrated in Fig. 8b. The increase of lateral soil stresses leads to the development of higher lateral loads in the case of dense sands.

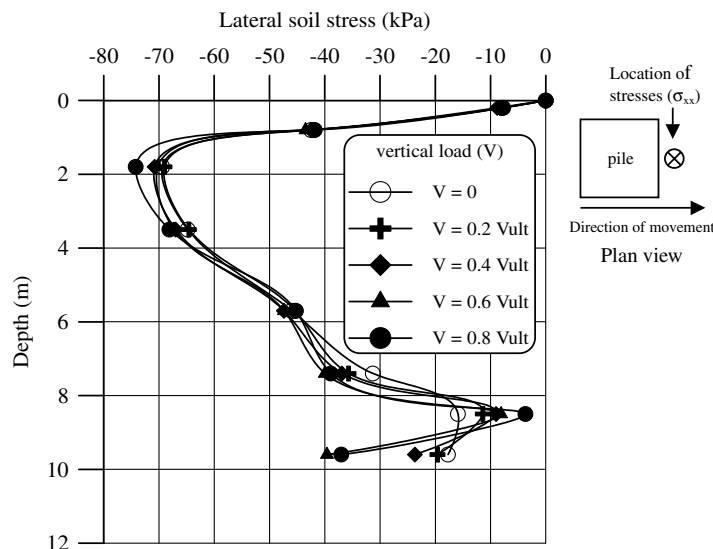


Fig. 8a. Variation of lateral soil stress (σ_{xx}) in front of the pile at a lateral deflection of 0.1B in loose sand.

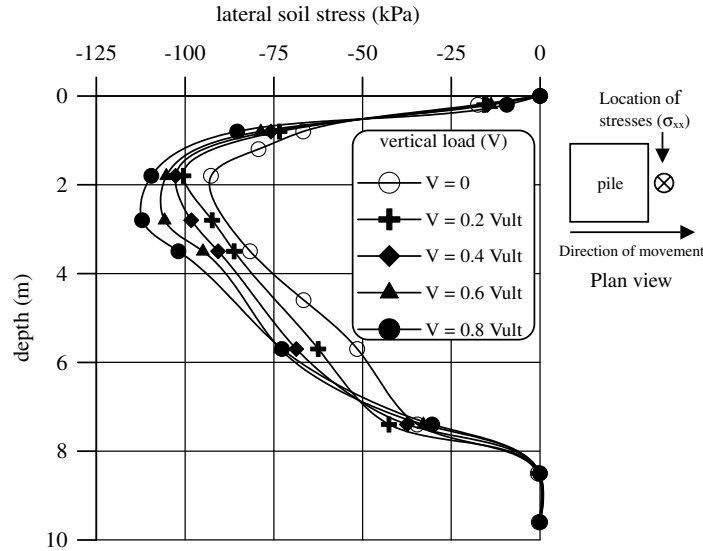


Fig. 8b. Variation of lateral soil stress (σ_{xx}) in front of the pile at a lateral deflection of 0.1B in dense sand.

The influence of vertical loads on the lateral deflections along the length of the pile reveal similar behaviour for loose and dense sands as illustrated in Figs. 9 and 10. The lateral deflections in the loose sand case are at lateral load level of 398 kN, and those in dense sand are at 641 kN. These loads correspond to a lateral deflection of 0.1B under pure lateral load for loose and dense sands, respectively. It is clear that the vertical loads have very little influence on the lateral deformations in the case of loose sands. The point at which the pile rotates is also not influenced by the vertical loads in the case of loose sands. On the other hand, the lateral deflections have reduced considerably due to the presence of vertical loads in the case of dense sands. The point of rotation has also moved up as the vertical load levels increase in the case of dense sands.

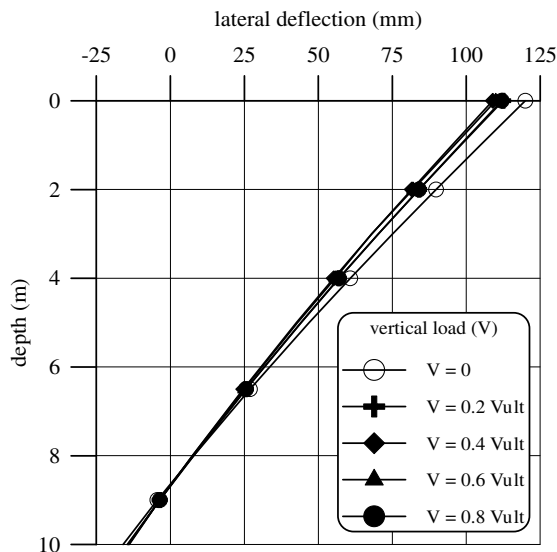


Fig. 9. Influence of vertical load on the variation of lateral deflection along the length of the pile in loose sand.

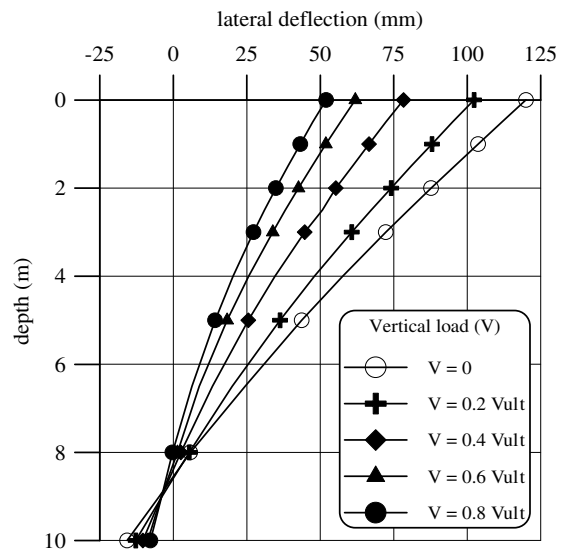


Fig. 10. Influence of vertical load on the variation of lateral deflection along the length of the pile in dense sand.

The data on lateral deflections clearly shows the influence of vertical loads on the lateral behaviour of piles.

The contours of lateral soil stresses (σ_{xx}) developed in dense sand under different vertical load levels are shown in Fig. 11(a)–(e). These contours are plotted at a lateral deflection equal to 0.1B and at a depth of 3 m from the ground surface where the lateral soil stresses are highest as illustrated in Fig. 8b. It can be observed that as the vertical load levels increases, the lateral soil stresses also increase around the pile. The increase in the size of the zone of influence around the pile at higher vertical load levels can also be observed from these figures.

From the above discussions, it is clear that the influence of vertical load on the lateral response of piles is more prominent for dense sands than loose sands. The reasons

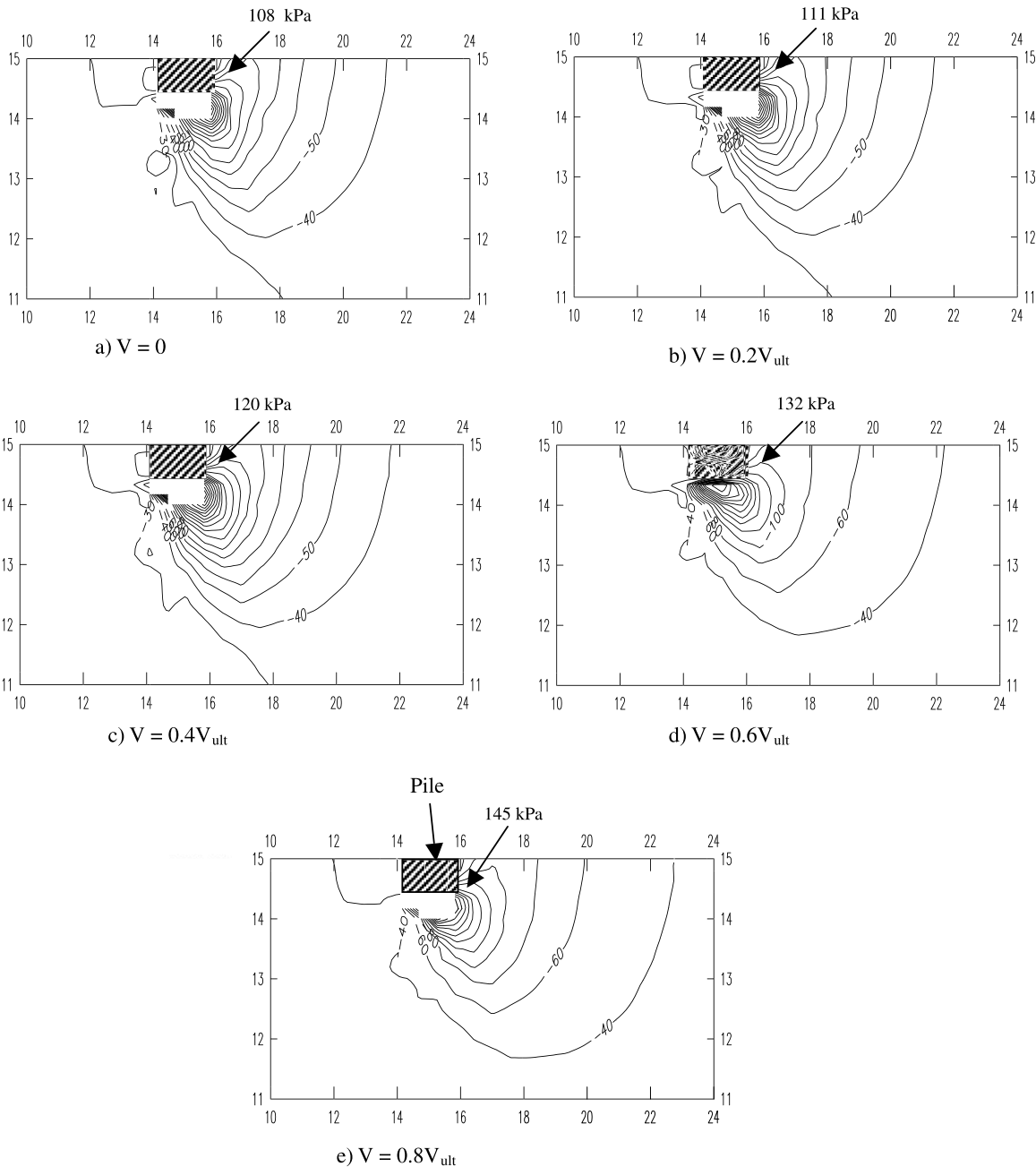


Fig. 11. (a–e) Contours of lateral stress (σ_{xx}) at a pile deflection of $0.1B$ and different vertical load levels.

for the difference in behaviour is further assessed through the following factors such as angle of internal friction, dilation angle and soil modulus. The influence of soil modulus and the angle of internal friction are illustrated through Fig. 12, which shows the response of pile under pure lateral load case together with one vertical load equal to $0.6V_{ult}$. The Percentage Improvement in lateral Capacity (PIC) due to the presence of vertical loads was significant with respect to the difference in friction angle (30° and 36°). However, the behaviour is found to be nearly the same for a soil having friction angle of 36° and different Young's modulus values of 20 and 50 MPa. Similarly, the influence of the dilation angle (ψ) has been separately studied by

varying ψ from zero to a maximum value of $\phi/3$ (i.e., 10° in the case of loose sands and 12° in the case of dense sands). Fig. 13 shows the variation of the Percentage Improvement in lateral Capacity (PIC) for different dilation angles. It can be seen that the PIC is also dependent on the dilation angles, however the percentage improvement is much less for loose sands as compared to dense sands.

6. Influence of pile head fixity

As the previous results have clearly shown that the influence of vertical load is more prominent in the VPL case and dense sands, the influence of pile head fixity was studied

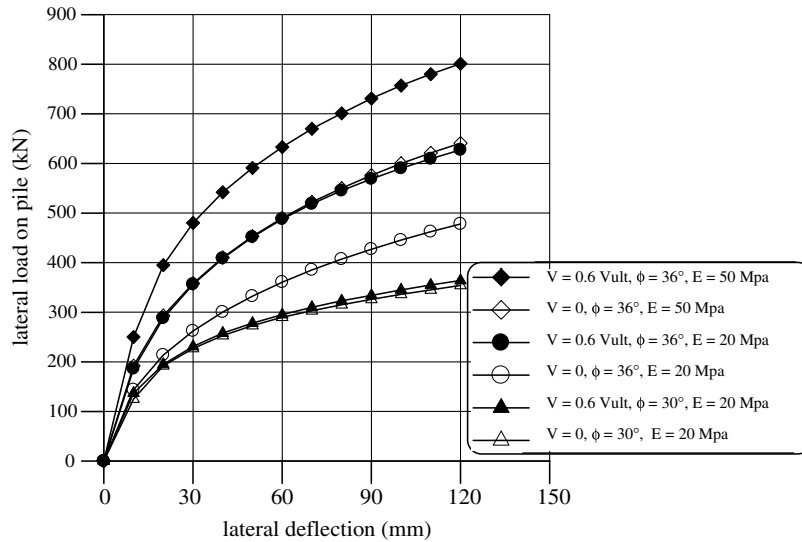


Fig. 12. Influence of vertical load on the lateral response of pile with different soil modulus values and angle of internal friction.

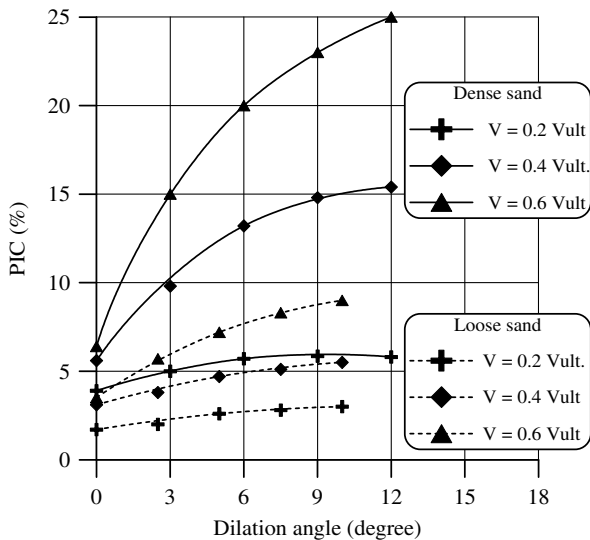


Fig. 13. Influence of dilation angle on PIC of pile in dense and loose sands.

only for the VPL case and in dense sand. To study the effect of pile head fixity, analyses were performed for free head and fixed head cases. For simulating the free head case, the pile head was allowed to rotate freely during the application of lateral deformations. In the fixed head case, the

pile head was not allowed to rotate by constraining the vertical deformations of nodes on the pile head to be the same during the application of lateral deformations. From the lateral load deflection curves, the Percentage Improvement in lateral Capacity (PIC) was assessed at different deflection levels of both the free head and fixed head piles under different vertical load levels and are summarized in Table 4. It can be observed that the lateral loads developed are higher for the fixed head than for the free head case. This is observed to be true even in the presence of vertical load. In general, the PIC value decreases at higher lateral deformations for both the free and fixed head cases. The reason for higher lateral loads for the fixed head case could be attributed directly to the restraint at the pile top. Besides, this phenomenon has been explained through the higher lateral soil stresses developed in front of the pile for the fixed head case, Fig. 14. It could be noted that the lateral stresses are more sensitive to vertical loads in the free head case than the fixed head case. The Percentage Increase in lateral soil Stress (PIS) may be defined as,

$$PIS = \frac{LSWV - LSNV}{LSNV} \times 100,$$

where, ‘LSWV’ is the lateral soil stress in front of the pile with vertical load and ‘LSNV’ is the lateral soil stress for the case of pure lateral load (no vertical load). Fig. 14 shows

Table 4
Percentage improvement in the lateral capacity (PIC) with respect to pile head conditions

Vertical load in terms of V_{ult}	Lateral load at deflection of 0.05B		PIC at deflection of 0.05B		Lateral load at deflection of 0.1B		PIC at deflection of 0.1B	
	Free head	Fixed head	Free head	Fixed head	Free head	Fixed head	Free head	Fixed head
0	453	1103	–	–	641	1847	–	–
0.2	486	1138	+7.3	+3.1	678	1872	+5.8	+1.3
0.4	547	1205	+20.7	+9.2	740	1926	+15.4	+4.3
0.6	591	1293	+30.4	+17.2	801	2000	+24.9	+8.3
0.8	631	1383	+39.3	+25.4	857	2081	+33.7	+12.7

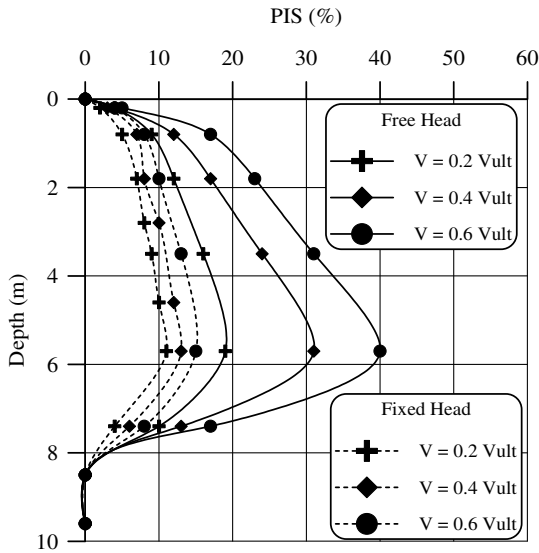


Fig. 14. Percentage Increase in lateral soil Stresses (PIS) in front of the pile with respect to pile head conditions.

the PIS values for free and fixed head piles. It is seen that PIS values for free head piles are higher than those for fixed head piles. The reason could be directly attributed to lower vertical stresses in fixed head piles than in the free head piles.

6.1. Influence of slenderness ratio of piles

To study this effect, a series of three-dimensional finite element analyses have been carried out considering 600 × 600 mm size piles and varying lengths of 5, 10 and 15 m in dense sand. Fig. 15 shows typical load–deflection relationships for three different L/B ratios (8.3, 16.7, and 25) with reference to pure lateral loads and under the influence of one typical vertical load ($V = 0.6V_{ult}$). It can be noted from the figure that the lateral load capacity of a pile

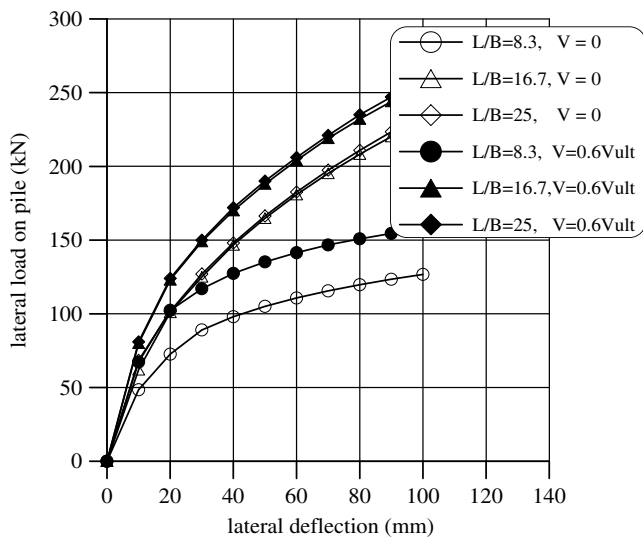


Fig. 15. Influence of vertical load on the lateral response of piles with respect to different L/B ratios.

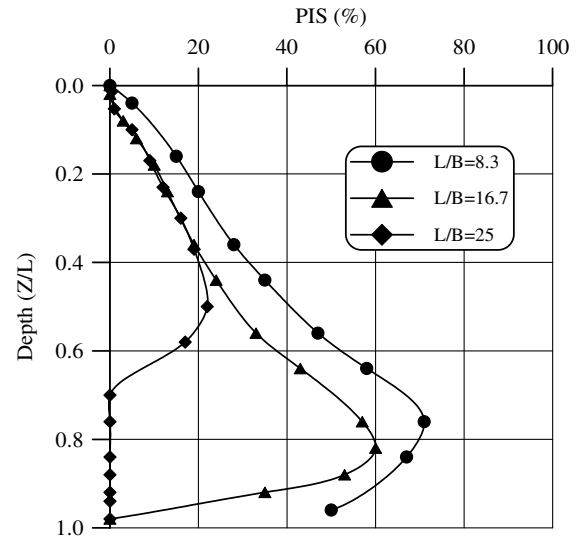


Fig. 16. Percentage Increase in lateral soil Stresses (PIS) in front of the pile with respect to different L/B ratios.

increases as L/B increases in all the cases. It is interesting to note that the influence of vertical load on the lateral response of piles decreases as the length of the pile (slenderness ratio) increases. The influence of vertical loads can be noted to be the highest for a short pile. The reasons for this could be attributed to the relatively higher Percentage Increase in lateral soil Stress (PIS) for short piles as compared to longer piles, as illustrated in Fig. 16.

7. Conclusions

Based on the results obtained in this investigation, the following conclusions can be made related to the influence of vertical load on the lateral response of piles.

1. The vertical load has a significant influence on the lateral response of piles embedded in sand. However, the influence depends on the sequence of loading, the soil parameters (angle of internal friction, dilation angle and soil modulus), the pile head fixity and the slenderness ratio (L/B).
2. When the vertical load is applied simultaneously with the lateral load (the SAVL case), the influence is felt only at greater deflection levels, whereas the influence is considerable at almost all the deflection levels when the vertical load is applied prior to the lateral load (the VPL case). In general, the influence of vertical load on the lateral response of the pile is less in the SAVL case.
3. The maximum Percentage Improvement in lateral Capacity (PIC) is up to 2.5% in loose sands and 12% in dense sands for piles in the SAVL case. On the other hand, there is significant improvement at deflection levels even up to 14.2% in loose sands and 39.3% in dense sands for piles in the VPL case. This is attributed to the development of additional lateral soil stresses in front of the pile and additional frictional resistance developed along its length.

4. In general, the Percentage Improvement in lateral Capacity (PIC) due to the presence of vertical load depends mainly on the soil parameters viz., the angle of internal friction and dilation angle and to some extent on the soil modulus.
5. The influence of vertical load on the lateral response of a pile is equally significant both in free head and fixed head piles; however, the influence is less in the case of fixed head piles in comparison to free head piles especially at larger deformation levels.
6. The influence of vertical loads is less significant in the case of long flexible piles. The reasons for this could be attributed to the relatively higher Percentage Increase in lateral soil Stress (PIS) in case of the short piles as compared to longer piles.

Acknowledgements

The authors would like to thank the Director, CBRI for the encouragement and interest in this research work. The first author is also thankful to the Director, CBRI for the leave sanctioned to pursue his doctoral research as an External Ph.D. scholar at IIT Madras, Chennai.

References

- [1] Anagnostopoulos C, Georgiadis M. Interaction of axial and lateral pile responses. *J Geotech Eng* 1993;119(4):793–8. ASCE.
- [2] Bartolomey AA. Experimental analysis of pile groups under lateral loads. In: *Proceedings of the Special Session 10 of the Ninth Int. Conf. on Soil Mech. and Foundation Engineering*. Tokyo, 1977;187–188.
- [3] Bowles JE. *Foundation analysis and design*. fourth ed. New York, USA: McGraw Hill company; 1988.
- [4] Brown DA, Shie CF. Some numerical experiments with a three-dimensional finite element model of a laterally loaded pile. *J Comput Geotech* 1991;12:149–62.
- [5] Comodromos EM. Response prediction for horizontally loaded pile groups. *J Geotech Eng Southeast Asian Geotech Soc* 2003;123–33.
- [6] Davisson MT, Robinson KE. Bending and buckling of partially embedded piles, *Sixth Int. Conf. on Soil Mech. and Foundation Engineering*, Montreal 1965;2:243–246.
- [7] Goryunov BF. Discussion on analysis of piles subjected to the combined action of vertical and horizontal Loads. *J Soil Mech Foundation Eng* 1975;10(1):10.
- [8] Hong SH, Lee FH, Yong KY. Three-dimensional pile–soil interaction in soldier-piled excavations. *J Comput Geotechn* 2003;30:81–107.
- [9] Jain NK, Ranjan G, Ramasamy G. Effect of vertical load on flexural behaviour of piles. *Geotech Eng* 1987;18:185–204.
- [10] Karasev OV, Talanov GP, Benda SF. Investigation of the work of single situ-cast piles under different load combinations. *J Soil Mechanics and Foundation Engineering (Translated from Russian)* 1977;14(3):173–7.
- [11] Kimura M, Adachi T, Kamei H, Zhang F. 3-D finite element analyses of the ultimate behaviour of laterally loaded cast-in-place concrete piles. In: *Proc. of the 5th Int. Symp. on Num. Models in Geomechanics*, 1995, Balkema, Rotterdam, p. 589–94.
- [12] Matlock H, Reese LC. Generalized solutions for laterally loaded piles. *J Soil Mech Found Division, ASCE* 1960;86(SM5):63–89.
- [13] McNulty JF. Thrust loading on piles. *J Soil Mech Found Div, ASCE* 1956;82(SM2):1–25.
- [14] Muqtadir A, Desai CS. Three-dimensional analysis of a pile group foundation. *Int J Num Anal Meth Geomech* 1986;39(1):97–111.
- [15] Nayak GC, Zienkiewicz OC. Elasto-plastic stress analysis: generalisation for various constitutive relations including strain softening. *Int J Num Meth Eng* 1972;5:113–35.
- [16] Poulos HG. Behaviour of laterally loaded piles: I-single piles. *J Soil Mech Found Div, ASCE* 1971;97(5):711–31.
- [17] Poulos HG, Davis EH. *Pile foundation analysis and design*. New York: John Wiley and Sons; 1980.
- [18] Ramaswamy G. Flexural behaviour of axially and laterally loaded individual piles and group of piles, Thesis submitted to Indian Institute of Science for the award of Ph.D. degree 1974; Bangalore.
- [19] Sorochan EA, Bykov VI. Performance of groups of cast-in place piles subjected to horizontal loading. *J Soil Mech Found Eng (Translated from Russian)* 1976;13(3):157–61.
- [20] Trochanis AM, Bielak J, Christiano P. Three-Dimensional Nonlinear Study of Piles. *J Geotech Eng, ASCE* 1991;117(3):429–47.
- [21] Wakai A, Ugai K, Gose S. The 3-D FE analysis of model group piles embedded in sand. In: *Proc. of 5th Int. Symp. on Num. Models in Geomechanics*, 1995, Balkema, Rotterdam, p. 613–8.
- [22] Wakai A, Gose S, Ugai K. 3-D elasto-plastic finite element analyses of pile foundations subjected to lateral loading. *J Soil Found* 1999;39(1):97–111.
- [23] Yang Z, Jeremic B. Numerical analysis of pile behaviour under lateral loads in layered elastic-plastic soils. *Int J Num Anal Meth Geomech* 2002;26:1385–406.
- [24] Zhukov NV, Balov IL. Investigation of the effect of a vertical surcharge on horizontal displacements and resistance of pile columns to horizontal loads. *J Soil Mech Found Eng (Translated from Russian)* 1978;15(1):16–21.